

Snack food as a modulator of human resting-state functional connectivity

Andrea Mendez-Torrijos,¹ † Silke Kreitz,¹ † Claudiu Ivan,¹ Laura Konerth,¹
Julie Rösch,² Monika Pischetsrieder,³ Gunther Moll,⁴ Oliver Kratz,⁴
Arnd Dörfler,² Stefanie Horndasch,⁴ and Andreas Hess^{1*}

¹ Institute of Experimental and Clinical Pharmacology and Toxicology, Emil Fischer Center, University of Erlangen-Nuremberg, Erlangen, Germany

² Department of Neuroradiology, University of Erlangen-Nuremberg, Erlangen, Germany

³ Department of Chemistry and Pharmacy, Food Chemistry Division, Emil Fischer Center, University of Erlangen-Nuremberg, Erlangen, Germany

⁴ Department of Child and Adolescent Mental Health, University Hospital of Erlangen, Erlangen, Germany

Objective. To elucidate the mechanisms of how snack foods may induce non-homeostatic food intake, we used resting state functional magnetic resonance imaging (fMRI), as resting state networks can individually adapt to experience after short time exposures. In addition, we used graph theoretical analysis together with machine learning techniques (support vector machine) to identifying biomarkers that can categorize between high-caloric (potato chips) vs. low-caloric (zucchini) food stimulation.

Methods. Seventeen healthy human subjects with body mass index (BMI) 19 to 27 underwent 2 different fMRI sessions where an initial resting state scan was acquired, followed by visual presentation of different images of potato chips and zucchini. There was then a 5-minute pause to ingest food (day 1 = potato chips, day 3 = zucchini), followed by a second resting state scan. fMRI data were further analyzed using graph theory analysis and support vector machine techniques.

Results. Potato chips vs. zucchini stimulation led to significant connectivity changes. The support vector machine was able to accurately categorize the 2 types of food stimuli with 100% accuracy. Visual, auditory, and somatosensory structures, as well as thalamus, insula, and basal ganglia were found to be important for food classification. After potato chips consumption, the BMI was associated with the path length and degree in nucleus accumbens, middle temporal gyrus, and thalamus.

Conclusion. The results suggest that high vs. low caloric food stimulation in healthy individuals can induce significant changes in resting state networks. These changes can be detected using graph theory measures in conjunction with support vector machine. Additionally, we found that the BMI affects the response of the nucleus accumbens when high caloric food is consumed.

Received 6 September 2017; Accepted 27 November 2017; First published online 4 April 2018

Key words: Food intake, graph theory, resting state networks, RS-fMRI, snack food, support vector machine.

Introduction

Pursey *et al.*¹ found that the prevalence of food addiction is around 20% in the Western world population. It is well known that food components and diets can modulate brain

functionality and brain activity,^{2,3} while the brain's activity patterns influence the quality and the quantity of nutritional intake^{4,5}. However, the nature of this relationship is unclear. Our early studies done on rats showed that specifically the mixture of 35% fat and 50% carbohydrate rather than the pure energy content in food leads to hedonic hyperphagia.^{6,7} Hedonic hyperphagia is described as caloric hyperalimentation beyond satiety.⁸ Humans also show preference to refined foods with high fat, sugar, or salt content, in quantities that show abuse and addictive-like behaviors.⁹ These high caloric foods, such as potato chips, are often consumed for reward and pleasure and not for homeostatic purposes. Furthermore, Schulte *et al.*¹⁰ assessed among 518 participants a list of 35 foods and their likelihood to be addictive. From their results, the

* Address for correspondence: Prof. Andreas Hess, Institut für Pharmakologie und Toxikologie, Fahrstraße 17, 91054 Erlangen (Deutschland).

(Email: Andreas.Hess@fau.de)

† These authors contributed equally.

We would like to thank all the participants of the study. We would also like to thank the excellent technical support in the Neuroradiology Department of the FAU, as well as Jutta Prade and Marina Sergeeva from the Institute of Experimental and Clinical Pharmacology and Toxicology.

This project was supported by the Neurotrition Project by FAU Emerging Fields Initiative.

snack food potato chips turned out to be the third most likely addictive food.

Functional magnetic resonance imaging (fMRI) studies, being the gold-standard for non-invasively investigating human brain functions, have highlighted the existence of brain anomalies and vulnerability factors related to obesity and eating disorders such as binge eating or anorexia nervosa.^{11–15} fMRI is expanding our knowledge on the neurobehavioral dimensions of food choices and motivation processes. For example, one study reported that in humans, pleasantness of a food is highly correlated with whether it will be eaten and how much will be eaten.¹⁶ A different study identified the primary gustatory cortex in the anterior insula of human subjects with the quality and intensity of taste. The orbitofrontal cortex and anterior cingulate cortex were also found to represent the reward value of taste; activations in this area correlate with the subjective pleasantness of taste.^{17,18} Another neuroimaging study suggested that the ventromedial prefrontal cortex (vmPFC) is in charge of short-term value of stimuli (eg, taste), whereas the dorsolateral prefrontal cortex (DLPFC) is in charge of long-term considerations (eg, health). The researchers concluded that failed self-control in obesity can be dependent on the extent to which the DLPFC can modulate the vmPFC.¹⁹ These neuroimaging findings pave the way to prevention studies that could help early diagnostics and better treatment options for eating disorders. However, the exact neuronal mechanisms underlying these disorders remain unclear.

Recently, neuroimaging interest has been directed toward spontaneous brain activity in the absence of a task or stimulus, the so-called resting state fMRI (RS-fMRI).²⁰ The results are different spatial patterns of functionally connected brain structures that are referred to as resting state networks (RSNs). A variety of these networks have been identified as behavior driving.²¹ It has been proven that RSNs can individually adapt to experience after short-time exposures to a stimulus, and these RSNs are a good indicator for addictive behaviors.^{22,23} Furthermore RS-fMRI has proven to work as an early indicator of neurological and psychiatric disorders due to pathological changes in the brain.^{24,25}

Graph theoretical analyses consider the whole brain dynamics and have been proven effective in detecting abnormalities of RSNs.^{26–28} Graph theory (GT) describes the whole brain as an interrelated network and quantifies this network organization, like the information flow, using different measures.²⁹ Additionally, support vector machines (SVM) are one of the most robust tools used in machine learning because of their ability to discriminate a set of features between (2) categories in high dimensional spaces, and an excellent reproducibility of the classification results.^{30,31} Used in conjunction with GT, SVM provides new insights in understanding brain dynamics.^{27,32–34}

The current study aimed to determine whether visualization followed by ingestion of different food types (high-caloric: potato chips, and low-caloric: zucchini) is able to generate different changes in the resting state networks of healthy individuals. In addition, we propose a method using graph theoretical analysis in conjunction with SVM for identifying biomarkers that can differentiate the 2 types of food stimulation.

Methods

Participants

A total of 19 (10 female, 9 male) healthy right-handed participants with body mass index (BMI) in the range 19–27 and aged 26–47 were recruited from the research staff of the Friedrich-Alexander-Universität Erlangen-Nürnberg (FAU). Participants did not receive financial compensation. Exclusion criteria included absence of any current or past form neurological/psychiatric diseases, having a BMI outside the range of 19–27, or having any contradictions to fMRI scanning. Ethical approval (220_15B) was provided by the local ethics committee of FAU, and informed consent was obtained from all participants. The study adhered to the tenets of the Declaration of Helsinki.

Study design

The experimental procedures are summarized in Figure 1. Every subject underwent 2 different fMRI sessions of ~40 minutes in total. The interval between the 2 sessions was 3 days. Participants arrived to the university clinic previously knowing what food they would be presented each day. The intention behind this was to increase the expectation of food reward, which is known to enhance neural cue reactivity.³⁵ The subjects were asked not to eat food for at least 2 hours before the experiment. At arrival, participants filled out a questionnaire and subsequently entered the MRI scanner. In each session, resting state was measured twice by instructing the participants to rest with their eyes open and lay still in an ambient light environment. Each fMRI session started by acquiring the individual anatomical imaging, followed by the first resting state (RS) scan (Pre RS-fMRI) and BOLD visual stimulation [presentation of different images of potato chips and zucchini: image presentation: total 196 vol. (time points) = 28 × 7, 1 block of images contained 7 images, 1 image = 1 vol. = 3 sec)]. There was then a pause of 5 minutes, where the participants were moved out of the scanner but remained on the motor table and had to consume (day 1 = salted potato chips: 528 kcal/100 g, 33% fats, 49% carbohydrates; day 3 = sliced zucchini: 17 kcal/100 g, 3% fats, 3.5% carbohydrates) ad libitum for 2 minutes. They were then introduced once again in the scanner for a second RS scan (Post RS-fMRI). [Note: The

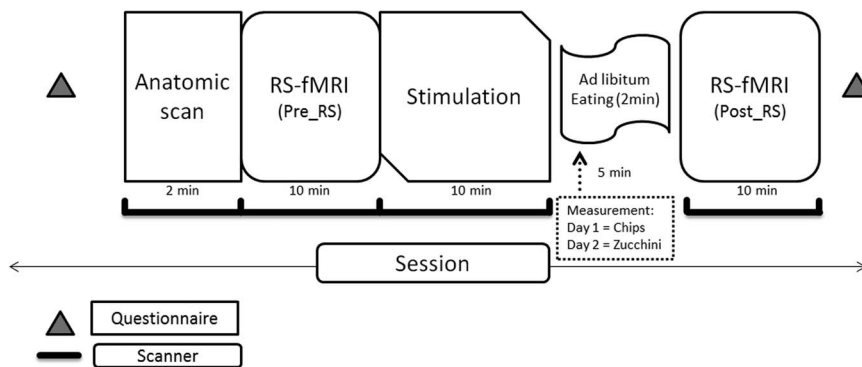


FIGURE 1. Schematic of the study protocol.

results of the BOLD stimulation and questionnaire results are beyond the scope of the current publication.]

The MRI data were collected by a 3T scanner (Magnetom trio; Siemens) using a standard 8-channel, phased-array head coil. For anatomic datasets, a T1-weighted, magnetization-prepared, rapid gradient-echo (standard Siemens MP-RAGE) sequence with 1 mm isotropic resolution was used; functional data were acquired using a standard single-shot, echo-planar imaging (EPI) sequence [repetition time/echo time (TR/TE) = 3000/30 ms] using a 128×128 matrix and a spatial resolution of 1.5 mm in plane, 3 mm slice thickness, and 0.75 mm gap between slices.

Data processing and analysis

The RS-fMRI data were analyzed initially for each subject, session, and measurement by means of BrainVoyager QX (v. 2.8, Brain Innovation B.V. Maastricht, The Netherlands). Our brain atlas of choice was the Harvard-Oxford brain atlas (<http://www.fmrib.ox.ac.uk/fsl/>), which is a set of probabilistic atlases covering 48 cortical and 21 subcortical structural areas. This atlas was used to define the different regions of interest (ROIs) necessary for the multi-seed region analysis, which preceded GT.

The next step was to preprocess the RS-fMRI data in BrainVoyager. Preprocessing of the anatomical data included inhomogeneity correction, brain extraction, spatial transformations, and selection of ROIs for white matter and ventricles. Inhomogeneity correction estimates the bias field of the B1 field of the receiver coil by analyzing the variability of white matter intensities over space.³⁶ The brain was then segmented from the skull and other head tissues using automatic “brain peeling.” This tool analyzes the local intensity histogram in small volumes ($20 \times 20 \times 20$ voxels) to define different thresholds for an adaptive region-growing technique.³⁷ The outcome was visually inspected and manually refined. Data were then transformed into anterior commissure - posterior commissure line and Talairach standard space (1mm³ isotropic). Finally ROIs were manually selected

for both white matter and ventricles and stored for later processing.

The preprocessing of functional data in BrainVoyager included slice scan time and head motion correction and a frequency space high pass filter on 0.009 Hz. Slice scan time correction was performed using sinc interpolation based on information about the TR (3000 msec) and the order of the slice scanning. 3D motion correction (trilinear and sinc interpolation) was carried out to detect and correct small head movements by spatially aligning all volumes of a subject to the first volume through rigid body transformations.³⁷ No spatial smoothing was performed at this stage. Due to software limitations of BrainVoyager QX 2.8, MagnAn (BioCom GbR, Uttenreuth, Germany) was used to perform the low-pass filter at 0.08 Hz, completing then the band-pass filter. The bandpass-filtered data were transferred back to BrainVoyager. Finally, a general linear model (GLM) was performed with the time courses from the previously selected ROIs (ie, white matter and ventricles) together with the motion correction predictors as cofounders. This was done to regress out these nonbrain function-related global fluctuations.

Connectivity analysis

Data were analyzed using BrainVoyager QX 2.8, Amira (FEI Company, OR, USA), and MagnAn. For the automatic multiseed coregistration method,³⁸ 48 cortical and 13 subcortical brain structures for each hemisphere were defined by registering (affine transformation with 9 degrees of freedom) the Harvard-Oxford 4D probability atlas to each dataset using BrainVoyager. This was done for all the individuals in all the different condition groups (pre RS-fMRI, post RS-fMRI for potato chips and zucchini sessions). Next, the seed regions were determined automatically through the center of mass of each of the identified atlas brain structures. The correlation was then calculated for all the voxels in the brain with the average time course of each seed region. Based on resulting 3D correlation volume map for

each seed region, the mean correlation value per brain structure was obtained by averaging over all significant correlating voxels of the given brain structure. By doing so, an asymmetric correlation matrix was generated with seed regions in rows and the correlating brain structures in columns.

Graph networks

In the next step, the resulting individual correlation matrices were transformed into network graphs consisting of vertices (or nodes) and edges. Vertices represent the brain's regions, whereas edges between pairs of brain regions indicate functional connectivity. The topology of network graphs is strongly dependent on the numbers of represented connections. The connections configuring a graph with a given sparsity were defined by thresholding (binarizing) the associated correlation matrix with the top 1230 number of connections [123 structures with an average number of edges (k) of 10]. The resulting network leads to different threshold values per matrix but of equal sparsity and therefore important to comparable graph topology.

Graph measures

The organization of complex networks can be characterized by various graph measures. These quantify the network's properties of integration and segregation and, therefore, are suitable to describe the efficiency of information flow within a network. Watts and Strogatz³⁹ were the first to characterize "small world network" topology. This was represented by the small world index (σ), which represents the effectiveness of the information flow, and is calculated as the quotient of the normalized clustering coefficient and the normalized average path length. To generate characteristic network features (network statistics per brain region), diverse graph

measures were calculated on the binarized matrices from the 2 post RS measurements for each brain structure per individual using MagnAn: path length, clustering coefficient (functional integration and functional segregation), and degree. The path length measures the average functional distance between 2 nodes, whereas the clustering coefficient is the tendency of network nodes to cluster.²⁹ A network with short path lengths and high clustering coefficient can be considered functionally integrated. On the other hand, long path lengths and low clustering coefficient is a sign of functional segregation.

Degree is a factor of local significance of nodes in network topology. In addition, hub and authority (local nodal measures) features were computed on the averaged individual correlation matrices for each post RS measurement to see the effect of the stimulation. Local nodal measures describe the properties of individual network elements and determine connectivity characteristics associated with these elements.⁴⁰ For hub identification we used the hyperlink-induced topic search (HITS).⁴¹ This algorithm assigns 2 scores for each node: its authority, which estimates the amount of valuable information a node holds, and its hub score, which measures how many highly informative or authoritative nodes are being pointed to by a node.⁴²

Significant differences network-based statistics

In order to be able to compare differences in network topologies across 2 experimental conditions, here potato chips vs. zucchini, we decided to study the changes in connectivity between each pair of nodes (Figure 2). To identify pairwise RS associations that are significantly different in relation to the ingested food, we implemented a modified version of the network-based statistics (NBS), first introduced by Zalesky *et al.*⁴³ NBS relies on the assumption that the group differences in single

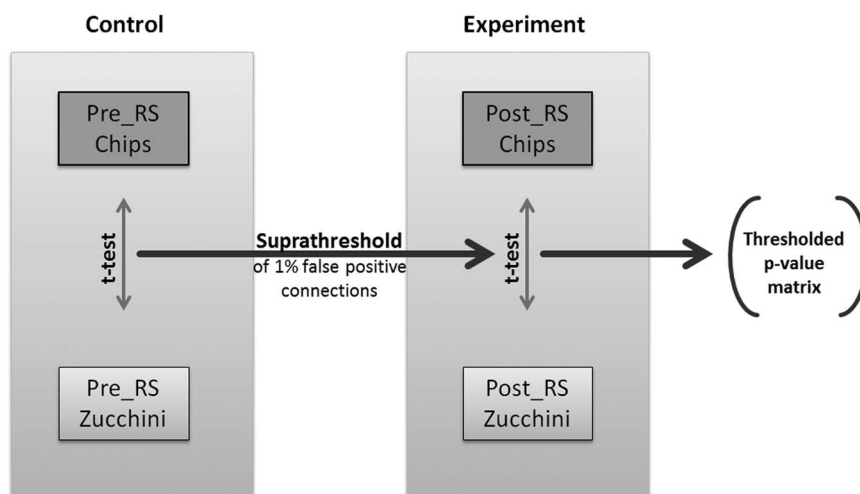


FIGURE 2. Flowchart of the applied paired Network Based Statistics approach.

connections are more likely to be false positive than the differences in larger connected components. To each connected component of group differences, a p-value, which controls for the family-wise error, was attributed using permutation testing.⁴³ However, experimental designs with paired subjects between groups cannot be permuted, as the subjects' affiliation to a group cannot be randomly changed. To overcome this limitation, we implemented an additional control experiment with identical experimental parameters. The pre-RS measurements for both food conditions were considered as the control experiment, as repeated RS measurements have been shown to be robust and stable.^{21,44–46} Our paired NBS approach used the Fisher's z-transformed correlation matrices of all 4 RS scans per individual (2 of the experimental and 2 of the control measurements). For each individual, the differences of correlation values per connection between the 2 RS correlation matrices of each session (control and experimental) were calculated. These difference matrices are used to calculate the pairwise t-statistics and later on the permutation testing. We then determined the 99% quantile of the p-values of the paired t-statistics of the control group and identified a set of supra-threshold links corresponding to 1% hypothetical false positive connections. This threshold was applied to the paired t-statistics p-values of the experimental group, and all connected components above this threshold that are equal or smaller than the largest component of the control group were eliminated. The remaining connected components of modulated connections were exclusively based on the connections that were part of RS graphs with defined sparsity (1230 strongest directed connections, see above).

Fisher score and SVM

For each brain structure, the 5 statistical parameters mentioned above (path length, clustering coefficient, degree, hub, and authority) were computed per RS measurement. Consequently, using all the brain structures (123 in total), we obtained a feature vector of 738 dimensions for each measurement.

Once the features were created, the high dimensionality became a problem. This is because when dimensionality increases, the volume of the space augments so fast that the data results become sparse. Sparsity is problematic for any method that requires statistical significance. In order to obtain a statistically reliable result, the amount of data needed to support the result often needs to grow exponentially with the dimensionality.⁴⁷ As a result, we employed a specific feature selection for dimensionality reduction. For this task we chose the Fisher score, which immediately allows the comparison of the discriminating power of the selected features, one by one, granting the possibility to choose

the features that would best classify the data while keeping their number to a minimum.^{27,31,48}

Support vector machines (SVMs) belong to the field of machine learning for 2-group classification problems. The selected features were mapped in a high m -dimensional space (m being the number of selected features). In this space a linear hyperplane classifier was constructed to robustly separate the groups.^{30,31,49} SVM analyses were conducted in Python (Python Software Foundation, <https://www.python.org/>) using the scikit-learn library (<http://scikit-learn.org/stable/>). To test the accuracy performance of the classification model, we employed leave-one-out cross-validation (LOOCV). LOOCV is a form of K -fold cross-validation, where K is equal to N (being in our case $N=32$, 2 measurements per subject).⁵⁰ The most discriminative features based on the Fisher scores were used to train the classifier. Using the LOOCV method, we aimed at evaluating the classifier's accuracy, specificity, and sensitivity. The number of selected features increased for each fold until all were considered, obtaining different accuracies for each run.^{27,51} We chose specificity as a measure to reflect the capacity of SVM to correctly classify potato chips stimulation and sensitivity to reflect the capacity to correctly classify zucchini stimulation. Moreover, we thereby identified the most discriminative brain regions related to specific graph measures, according to different cutoff scores.

In addition, Pearson correlation coefficients were calculated among potato chips post RS-fMRI graph measures and BMI, to check for the specific effect of high-caloric food stimulation. Linear regression models were used to determine significant associations ($p < 0.05$). Only degree and path length showed significant correlations with BMI. Therefore, we focused on these measures to investigate both local and global dynamics.

Results

The STROBE⁵² flowchart for recruitment is shown in Figure 3. One female participant was excluded from the analysis, as her fMRI data were corrupted. The final sample used for the complete analysis resulted in 16 (9 female and 7 male) healthy participants with BMI in the range 19–27 kg/m² (mean = 23 kg/m², SD = 2.6 kg/m²), aged 26–47 years (mean = 33 years, SD = 6.8 years).

In order to study how potato chips consumption after visual stimulation induces dynamic modulations in resting state connectivity as opposed to zucchini consumption, we performed 4 different kinds of analysis. First we checked for the global measure the small world index σ , as introduced in the Methods section as a measure of information flow (Figure 4). Results show that σ was preserved, as there were no significant differences between the different measures. For this

reason we conducted a more sophisticated analysis to understand the RSN differences. NBS and SVM are methods for characterizing networks with the advantage of not compressing all information into one single value.

Connectivity differences

Following, paired NBS was used to determine any significant changes between pairwise connectivity. For the statistical analysis, the difference matrices were used to calculate the uncorrected paired t-statistics. Compared to the control condition, the visual presentation

followed by the consumption of different food led to significant connectivity changes in the post resting state (both at $\alpha=0.0186$) with widespread significant differences between potato chips and zucchini (as illustrated in Figure 5). After thresholding the paired t-statistics p-values, a p-value controlling the family-wise-error was ascribed using permutation testing to each remaining connected component of group differences ($p=0.093$). These changes took place mainly between cortical structures, with the exception of the basal ganglia. Overall, the left hemisphere showed more connectivity changes, mainly decreased, than the right one. Three frontal nodes stood out among the rest: the inferior frontal gyrus, frontal orbital cortex, and planum polare, the pairwise connectivities of which mainly decreased for potato chips compared to zucchini. In contrast, the pairwise connectivity mostly increased for potato chips compared to zucchini between temporal structures, such as the planum temporale, inferior temporal gyrus, and temporal pole. The occipital area also showed changes in connectivity in both directions, increased and decreased.

Classifier accuracy

The SVM was calculated to detect the most discriminative structures and measures between potato chips and zucchini. Table 1 shows the classification, sensitivity, and specificity scores using LOOCV when comparing potato chips to zucchini consumption, when preceded by a visual presentation of both food items. The number of features that resulted in the best classifier performance depended on the desired cutoff score. As shown, 67

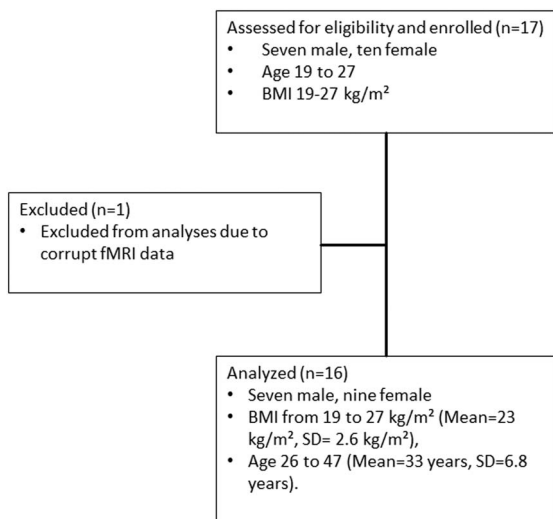


FIGURE 3. STROBE flowchart for recruitment.

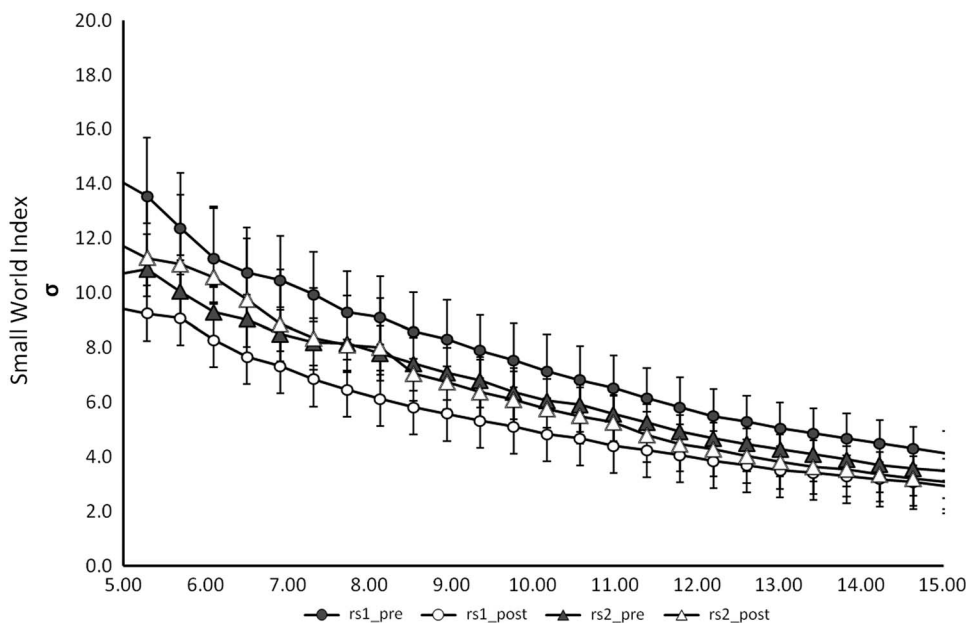


FIGURE 4. Graph representing the small world index for the different RS-fMRI measures against k (average number of connections per node). No significant differences were detected between the groups.

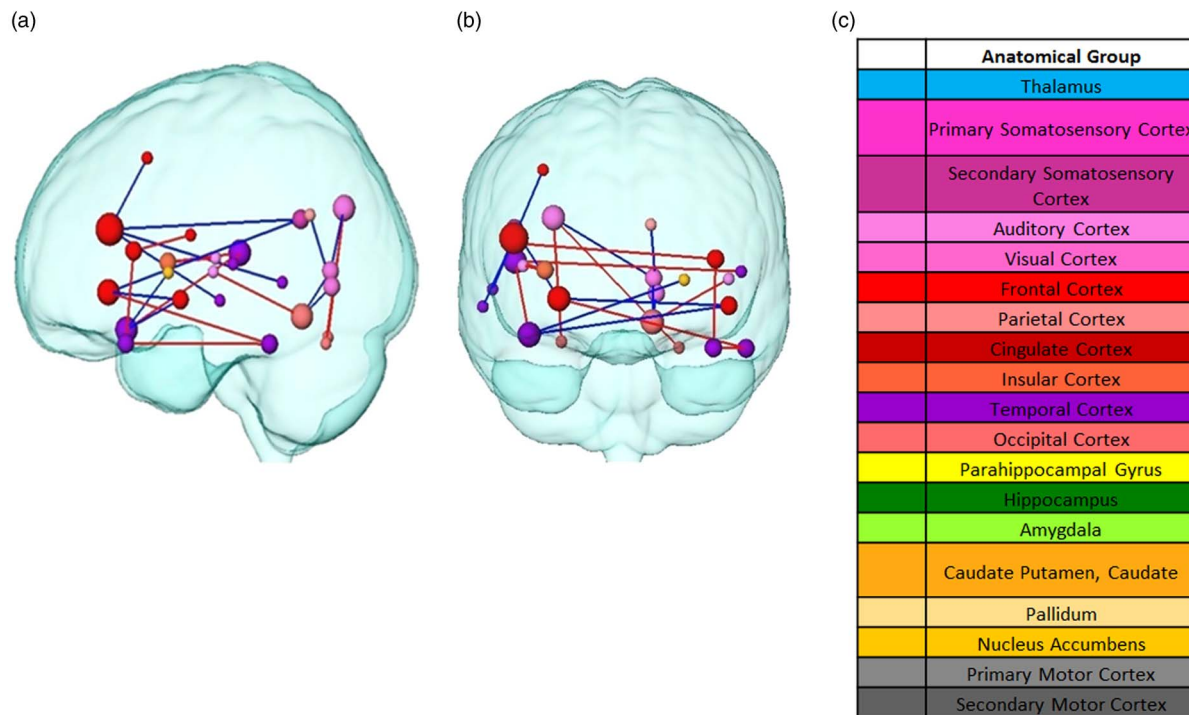


FIGURE 5. Pairwise connectivity differences between food stimuli from two different planes. (a) Sagittal view (b) Coronal plane. Node Red edges represent increased connectivity for chips compared to zucchini. Blue edges represent decreased connectivity for chips compared to zucchini. Colors correspond to the anatomical groups in the Harvard-Oxford brain atlas (c) Color label of the anatomical brain regions. Node size represents the total degree (total amount of connections with the rest of the network).

TABLE 1. Accuracy, sensitivity and specificity scores using LOOCV when comparing chips to zucchini stimulation

Cut-off	Number of features	Accuracy	Specificity	Sensitivity
0	67	100%	100%	100%
0.05	63	97%	100%	94%
0.1	38	91%	94%	88%
0.15	14	84%	81%	88%

features were needed to obtain the best classification performance with 100% of LOOCV classification accuracy.

Most selective features

For the identification of the most discriminative brain structures according to the graph theoretical measures, we selected the regions with 100% accuracy. Figure 6 and Table 2 illustrate the most discriminate features (cutoff of 0.15). Visual, auditory, and somatosensory structures were predominant. Various subcortical structures (thalamus, insula, and basal ganglia) were also found to play a role in discriminating between which food item had been consumed. Interestingly, results of our experimental design revealed changes mainly in left-sided brain regions.

BMI

Finally, we examined the relationship between BMI, degree, and path length after eating potato chips when preceded by the visual presentation of both food items through Pearson’s correlation coefficients. BMI was found to correlate significantly with degree and path length of several brain structures (see Table 3 and Figure 7). BMI was positively associated with the path length of the right middle temporal gyrus and bilateral nucleus accumbens, and negatively associated with the right premotor thalamus. Similar findings were obtained for BMI and degree. However, in this case, the right premotor thalamus was found to be positively associated, and the right temporal thalamus and bilateral nucleus accumbens was found to be negatively associated, meaning the higher the BMI, the fewer number of connections in the latter areas.

Discussion

This study shows that the combination of visualization and ingestion of different food types (potato chips and zucchini) leads to specific changes in resting state networks of healthy individuals. Interestingly, graph theoretical analysis in conjunction with SVM was able to discriminate with 100% accuracy between the effect of the 2 types of food consumption after subjects were primed with the visual presentation. Moreover, graph-

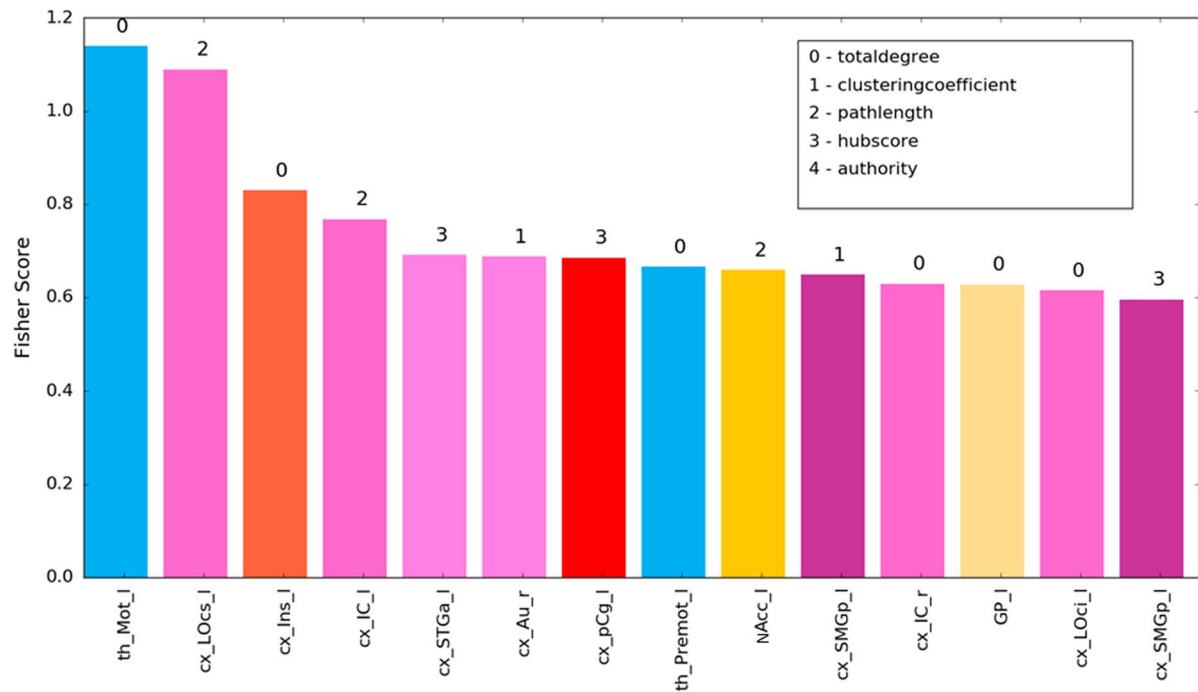


FIGURE 6. SVM of most discriminative features (cutoff 0.15) showing the fisher z-score for the individual brain structures. Bar colors correspond to labelling scheme given in Figure 4c.

TABLE 2. SVM's highest discriminative brain regions (cutoff 0.15) according to the Harvard-Oxford atlas

Abbreviation	Name in Harvard-Oxford Atlas
Th_mot_L	Primary motor thalamus
Cx_LOcs_L	Lateral occipital cortex, superior division
Ins_L	Insula
Cx_IC_L	Intracalcarine cortex
Cx_STGa_L	Superior temporal gyrus, anterior division
Cx_Au_R	Heschl's gyrus (includes H1 and H2)
Cx_pCg_L	Paracingulate gyrus
Th_premot_L	Pre-motor thalamus
Acc_L	Nucleus accumbens
Cx_SMGp_L	Supramarginal gyrus, posterior division
Cx_IC_R	Intracalcarine cortex
GP_L	Pallidum
Cx_LOci	Lateral occipital cortex, inferior division
Cx_SMGp_L	Supramarginal gyrus, posterior division

Note: L, left; R, right.

theoretical analyses illustrate differences at the connectivity and intra-node level of activation between the 2 types of food stimuli. Additionally, BMI should be considered when investigating the connectivity effects of high caloric foods.

The global assessment of the RSNs in terms of the small world index σ was proven insufficient for our study. Previous RS-fMRI studies using clinical populations found σ as an index for effectiveness of information flow in a network, which is valuable for differential diagnosis,

TABLE 3.

Anatomical label	Path length		Degree	
	r	p-value	r	p-value
Premotor thalamus right	-0.585	0.041*	0.675	0.016*
Temporal thalamus right	0.442	0.128	-0.612	0.031*
Middle temporal gyrus Right	0.571	0.046*	0.149	0.614
Nucleus accumbens right	0.648	0.022*	-0.689	0.014*
Nucleus accumbens left	0.678	0.016*	-0.626	0.027*

Note: r = Pearson correlation coefficient; *p < 0.05.

ie, Alzheimers, mild cognitive impairment.^{53,54} However, in normal functioning brain networks, as investigated here, a more detailed analysis is needed that does not compress the complexity of the information flow into a single value.

Using RS-fMRI derived measures and paired NBS, we created the brain's functional network connectivity. We found global connectivity differences between potato chips and zucchini compared to the pre-RS-fMRI condition. Connectivity of diverse frontal structures, especially the left frontal orbital cortex, mainly decreased for potato chips compared to zucchini. The frontal orbital cortex responds to visual presentations of food stimuli and plays a role in visual, olfactory, and taste representation, as well as in the evaluation of food reward.⁵⁵ One previous study found increased frontal orbital cortex activation when viewing low-caloric foods in comparison

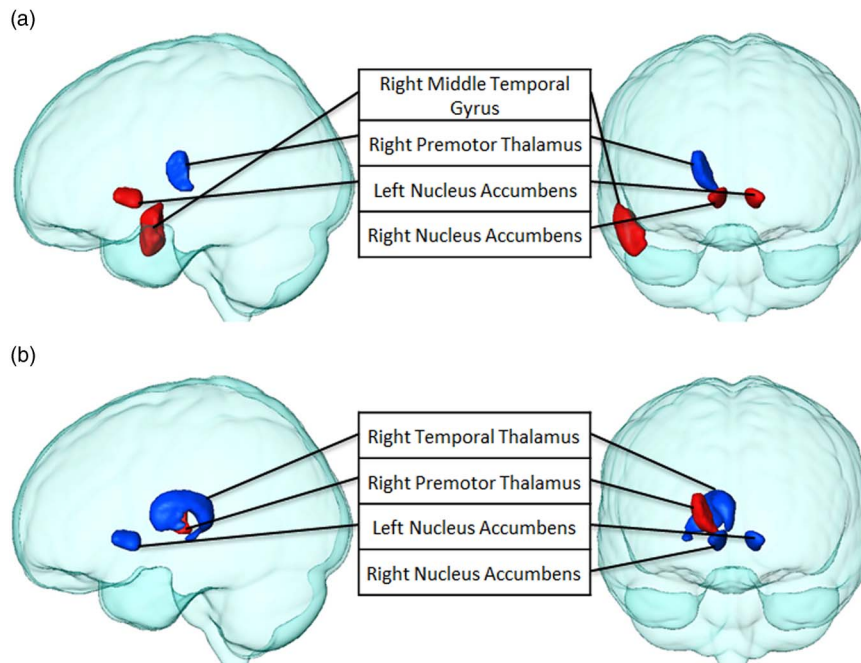


FIGURE 7. Brain structures that significantly correlate between BMI with (a) path length and (b) degree, after chips consumption ($p < 0.05$). Regions with positive correlations are highlighted in red, while negatively correlated regions are blue.

to high caloric foods.⁵⁶ The authors speculated about the possibility that association with reward of low strength (in our case zucchini) may require more extensive integrative processing in the frontal orbital areas. Food with lower reward value may have encouraged less effective responses throughout a lifetime.⁵⁷ Conversely, the frontal orbital cortex is also involved in representing negative reinforcements, such as aversive taste.⁵⁸ Our healthy participants may have found zucchini unpleasant, experiencing an aversive response to zucchini resulting in stronger frontal orbital connectivity. We specifically found decreased connectivity between the inferior frontal gyrus (frontal cortex) and the middle temporal gyrus (temporal cortex) for potato chips in comparison to the zucchini condition. The first region is related to associative and item recognition. Moreover, the connections with the middle temporal gyrus have been already described. The middle temporal gyrus supports the use of pre-experimental acquired associations during the retrieval efforts of the inferior frontal gyrus.⁵⁹ Zucchini might be a weaker stimulus than potato chips, and stronger retrieval efforts might be needed for its identification as a food item. Equally important is the increase of connectivity between temporal structures as well as the decrease of pairwise connectivity in frontal areas for chips in comparison to zucchini. These areas have not been previously associated with food processing; however, they comprise part of Wernicke's area, which is involved in semantic processing. The potato chips fMRI was the first session to take

place; therefore it is possible to speculate that the effects on the semantic processing of the visual categories were stronger during this session due to a novelty response.^{60,61} Furthermore, we found planum temporale activation which could be explained by the scanner's noise and its novelty effect during the first session.^{62,63}

Once food type differences after visual presentation were established though paired NBS, we used graph theoretical measures as discriminative features for automatically classifying individuals depending on the food received that day. SVM's best classification accuracy was achieved with 67 features. Consequently, the current study demonstrates an analysis method capable of distinguishing between the type of food received with an accuracy of 100%. It was shown that the lateral occipital cortex, insula, striatum (basal ganglia), and nucleus accumbens have a high sensitivity for food stimulus discrimination. These highly discriminative regions have been previously described in food-related research. The lateral occipital cortex has been proven to be related to the perception of emotionally salient stimuli like food, which can lead to increased attention.^{64,65} Consequently, potato chips might be more salient stimuli than zucchini or vice versa, proving the lateral occipital cortex as a critical brain region. The insula, being in our study partly responsible for the modulation of connectivity by different food, is involved in memory retrieval of previous experiences, including imagining the taste of food, craving for food, and the mouth feel of water and fat, and has been described in the context of eating

disorders and obesity.^{64,66–68} Among many functions, the ventral striatum has been related with the attribution of a superior metabolic reward value to high energy foods as compared to low energy foods.⁶⁹ Furthermore, one study related satiation with attenuated BOLD activity in the nucleus accumbens (ventral striatum).⁷⁰ In our study, the intake of zucchini might have resulted in lower food craving than potato chips intake due to its low reward value, being the striatum, and more concretely the nucleus accumbens a critical brain region for reward processing. Additionally, most discriminative brain structures were located in the left hemisphere. This effect was also seen for the pairwise connectivity, where most changes were also lateralized to the left. Our research evidenced that after attending food pictures and consuming food, a large network of left-sided brain regions is strongly activated. The involvement of these left brain areas in the explicit processing of food cues is in accordance with previous findings.^{56,66} Furthermore, all of our participants were right-handed. Different studies associated performance of a visual working memory task in right-handed participants with lateralization of brain activity in the left hemisphere.^{59,71}

Another key finding of this study is that when stimulated with the same food pictures followed by potato chips consumption, the degree and path length in certain areas were associated with BMI; particularly interesting is again the nucleus accumbens. A previous study related nucleus accumbens activation to the amount of fat consumed at a buffet.⁷² Furthermore, the nucleus accumbens contains opioid pathways that stimulate intake of highly palatable and energy-rich foods.⁷³ The structures of these pathways seem to increase their path length, being less globally efficient with increasing BMI. Moreover, part of our participants had a BMI higher than 25 kg/m², which can be considered slightly overweight. Scientists found that increased reward responsivity to food cues in the nucleus accumbens is associated with subsequent weight gain during the 6 following months,⁷⁴ and that overweight women have functional alterations within the nucleus accumbens.⁷⁵ On the other hand, the number of connections of the accumbens after potato chips consumption decreased with increasing BMI, again indicating less global interconnectivity. One study showed similar results, where dopamine release was reduced in the accumbens after calorie intake in obese subjects in contrast to healthy individuals.⁷⁶

Several limitations should be considered when interpreting the present findings. Unfortunately in this study there was no RS-fMRI measurement between the visual stimulation and the food consumption. Therefore individual effects of both components on the resting state networks could not be differentiated. Furthermore, an important covariate such as gender was not considered in

this study due to limited number of participants. Different studies stress the importance of sex differences in the response to satiation, suggesting that the regulation of food intake by the brain may vary depending on gender.^{71,77,78} A higher number of participants is recommended for future studies to avoid limited statistical power.⁷⁹ Furthermore, different studies identified the hypothalamus as the structure responsible for modulating food reward.^{80–82} Our atlas of choice, the Harvard-Oxford atlas, did not include the hypothalamus; therefore, this area was not considered during our analysis. The external validity of our results should also be taken into account, as our results are limited to the 2 food items of our choice. Furthermore, Western diets are different from diets of other regions, and therefore our food choice might not be translatable to other populations.¹⁰

Conclusions

Overall, this study determined that there are different changes in RSNs after visualizing and ingesting potato chips (high caloric) vs. zucchini (low caloric) food in healthy individuals. We proposed our method based on graph theoretical analysis in conjunction with SVM to distinguish between different types of food stimuli. Our results aim to understand how nutritional components and diets can specifically modulate brain functionality and brain activity. We found that BMI positively correlated with activity in the nucleus accumbens when consuming snack foods. Unraveling human eating behavior and its neuronal mechanisms is of high importance to understand food-related disorders and ultimately to develop targeted obesity prevention.

Disclosures

None of the authors had any conflicts of interest or financial ties related to this work.

REFERENCES:

1. Pursey KM, Stanwell P, Gearhardt AN, Collins CE, Burrows TL. The prevalence of food addiction as assessed by the Yale Food Addiction Scale: a systematic review. *Nutrients*. 2014; **6**(10): 4552–4590.
2. Small DM, Zatorre RJ, Dagher A, Evans AC, Jones-Gotman M. Changes in brain activity related to eating chocolate: from pleasure to aversion. *Brain*. 2001; **124**(Pt 9): 1720–1733.
3. Tillisch K, Labus J, Kilpatrick L, Jiang Z, Stains J, Ebrat B, et al. Consumption of fermented milk product with probiotic modulates brain activity. *Gastroenterology*. 2013; **144**(7): 1394–1401, e1391–e1394.
4. Gomez-Pinilla F. Brain foods: the effects of nutrients on brain function. *Nat Rev Neurosci*. 2008; **9**(7): 568–578.
5. Thomas MA, Ryu V, Bartness TJ. Central ghrelin increases food foraging/hoarding that is blocked by GHSR antagonism and attenuates hypothalamic paraventricular nucleus neuronal activation. *Am J Physiol Regul Integr Comp Physiol*. 2016; **310**(3): R275–R285.

6. Hoch T, Pischetsrieder M, Hess A. Snack food intake in ad libitum fed rats is triggered by the combination of fat and carbohydrates. *Front Psychol.* 2014; **5**: 250.
7. Hoch T, Kreitz S, Gaffling S, Pischetsrieder M, Hess A. Fat/carbohydrate ratio but not energy density determines snack food intake and activates brain reward areas. *Sci Rep.* 2015; **5**: 10041.
8. Sharma AM, Padwal R. Obesity is a sign—over-eating is a symptom: an aetiological framework for the assessment and management of obesity. *Obes Rev.* 2010; **11**(5): 362–370.
9. Gearhardt AN, Davis C, Kuschner R, Brownell KD. The addiction potential of hyperpalatable foods. *Curr Drug Abuse Rev.* 2011; **4**(3): 140–145.
10. Schulte EM, Avena NM, Gearhardt AN. Which foods may be addictive? The roles of processing, fat content, and glycemic load. *PLoS One.* 2015; **10**(2): e0117959.
11. Burger KS, Stice E. Elevated energy intake is correlated with hyperresponsivity in attentional, gustatory, and reward brain regions while anticipating palatable food receipt. *Am J Clin Nutr.* 2013; **97**(6): 1188–1194.
12. Volkow ND, Wang GJ, Telang F, Fowler JS, Thanos PK, Logan J, et al. Low dopamine striatal D2 receptors are associated with prefrontal metabolism in obese subjects: possible contributing factors. *Neuroimage.* 2008; **42**(4): 1537–1543.
13. Uher R, Murphy T, Brammer MJ, Dalgleish T, Phillips ML, Ng VW, et al. Medial prefrontal cortex activity associated with symptom provocation in eating disorders. *Am J Psychiatry.* 2004; **161**(7): 1238–1246.
14. Brooks SJ, O'Daly OG, Uher R, Friederich HC, Giampietro V, Brammer M, et al. Differential neural responses to food images in women with bulimia versus anorexia nervosa. *PLoS One.* 2011; **6**(7): e22259.
15. Frank GK. Advances from neuroimaging studies in eating disorders. *CNS Spectr.* 2015; **20**(4): 391–400.
16. Rolls ET. Taste, olfactory and food texture reward processing in the brain and the control of appetite. *Proc Nutr Soc.* 2012; **71**(4): 488–501.
17. Grabenhorst F, Rolls ET. Selective attention to affective value alters how the brain processes taste stimuli. *Eur J Neurosci.* 2008; **27**(3): 723–729.
18. Grabenhorst F, Rolls ET, Bilderbeck A. How cognition modulates affective responses to taste and flavor: top-down influences on the orbitofrontal and pregenual cingulate cortices. *Cereb Cortex.* 2008; **18**(7): 1549–1559.
19. Hare TA, Camerer CF, Rangel A. Self-control in decision-making involves modulation of the vmPFC valuation system. *Science.* 2009; **324**(5927): 646–648.
20. Lee MH, Smyser CD, Shimony JS. Resting-state fMRI: a review of methods and clinical applications. *AJNR Am J Neuroradiol.* 2013; **34**(10): 1866–1872.
21. Damoiseaux JS, Rombouts SA, Barkhof F, Scheltens P, Stam CJ, Smith SM, et al. Consistent resting-state networks across healthy subjects. *Proc Natl Acad Sci U S A.* 2006; **103**(37): 13848–13853.
22. Ma N, Liu Y, Li N, Wang CX, Zhang H, Jiang XF, et al. Addiction related alteration in resting-state brain connectivity. *Neuroimage.* 2010; **49**(1): 738–744.
23. Kelly C, Zuo XN, Gotimer K, Cox CL, Lynch L, Brock D, et al. Reduced interhemispheric resting state functional connectivity in cocaine addiction. *Biol Psychiatry.* 2011; **69**(7): 684–692.
24. Liu Y, Liang M, Zhou Y, He Y, Hao Y, Song M, et al. Disrupted small-world networks in schizophrenia. *Brain.* 2008; **131**(Pt 4): 945–961.
25. Zhao X, Liu Y, Wang X, Liu B, Xi Q, Guo Q, et al. Disrupted small-world brain networks in moderate Alzheimer's disease: a resting-state fMRI study. *PLoS One.* 2012; **7**(3): e33540.
26. dos Santos Siqueira A, Biazoli Junior CE, Comfort WE, Rohde LA, Sato JR. Abnormal functional resting-state networks in ADHD: graph theory and pattern recognition analysis of fMRI data. *BioMed Research International.* 2014; **2014**: 380531.
27. Khazae A, Ebrahimzadeh A, Babajani-Feremi A. Identifying patients with Alzheimer's disease using resting-state fMRI and graph theory. *Clin Neurophysiol.* 2015; **126**(11): 2132–2141.
28. van den Heuvel MP, Mandl RC, Stam CJ, Kahn RS, Hulshoff Pol HE. Aberrant frontal and temporal complex network structure in schizophrenia: a graph theoretical analysis. *J Neurosci.* 2010; **30**(47): 15915–15926.
29. Bullmore E, Sporns O. Complex brain networks: graph theoretical analysis of structural and functional systems. *Nat Rev Neurosci.* 2009; **10**(3): 186–198.
30. Cortes C, Vapnik V. Support-vector networks. *Machine Learning.* 1995; **20**(3): 273–297.
31. Quanquan G, Zhenhui L, Jiawei H. Generalized Fisher score for feature selection. Proceedings of the Twenty-Seventh Conference on Uncertainty in Artificial Intelligence; 2012; Barcelona, Spain.
32. Dosenbach NU, Nardos B, Cohen AL, Fair DA, Power JD, Church JA, et al. Prediction of individual brain maturity using fMRI. *Science.* 2010; **329**(5997): 1358–1361.
33. Sacchet MD, Prasad G, Foland-Ross LC, Thompson PM, Gotlib IH. Support vector machine classification of major depressive disorder using diffusion-weighted neuroimaging and graph theory. *Front Psychiatry.* 2015; **6**: 21.
34. Li Y, Qin Y, Chen X, Li W. Exploring the functional brain network of Alzheimer's disease: based on the computational experiment. *PLoS One.* 2013; **8**(9): e73186.
35. Malik S, McGlone F, Dagher A. State of expectancy modulates the neural response to visual food stimuli in humans. *Appetite.* 2011; **56**(2): 302–309.
36. Vaughan JT, Garwood M, Collins CM, Liu W, DelaBarre L, Adriany G, et al. 7T vs. 4T: RF power, homogeneity, and signal-to-noise comparison in head images. *Magn Reson Med.* 2001; **46**(1): 24–30.
37. Goebel R, Esposito F, Formisano E. Analysis of functional image analysis contest (FIAC) data with brainvoyager QX: from single-subject to cortically aligned group general linear model analysis and self-organizing group independent component analysis. *Hum Brain Mapp.* 2006; **27**(5): 392–401.
38. Kreitz S, de Celis Alonso B, Uder M, Hess A. A new analysis of resting state connectivity and graph theory reveals distinctive short-term modulations due to whisker stimulation in rats. *bioRxiv.* Preprint. DOI: 10.1101/223057.
39. Watts DJ, Strogatz SH. Collective dynamics of 'small-world' networks. *Nature.* 1998; **393**(6684): 440–442.
40. Rubinov M, Sporns O. Complex network measures of brain connectivity: uses and interpretations. *Neuroimage.* 2010; **52**(3): 1059–1069.
41. Flake GW, Lawrence S, Giles CL, Coetzee FM. Self-organization and identification of Web communities. *Computer.* 2002; **35**(3): 66–70.
42. Kleinberg JM. Authoritative sources in a hyperlinked environment. *Journal of the ACM.* 1999; **46**(5): 604–632.
43. Zalesky A, Fornito A, Bullmore ET. Network-based statistic: identifying differences in brain networks. *Neuroimage.* 2010; **53**(4): 1197–1207.
44. Braun U, Plichta MM, Esslinger C, Sauer C, Haddad L, Grimm O, et al. Test-retest reliability of resting-state connectivity network characteristics using fMRI and graph theoretical measures. *Neuroimage.* 2012; **59**(2): 1404–1412.
45. Chen S, Ross TJ, Zhan W, Myers CS, Chuang KS, Heishman SJ, et al. Group independent component analysis reveals consistent resting-state networks across multiple sessions. *Brain Res.* 2008; **1239**: 141–151.
46. Smith SM, Beckmann CF, Ramnani N, Woolrich MW, Bannister PR, Jenkinson M, et al. Variability in fMRI: a re-examination of inter-session differences. *Hum Brain Mapp.* 2005; **24**(3): 248–257.

47. Bellman RE. *Dynamic Programming*. Mineola, New York: Dover Publications; 2003.
48. He X, Cai D, Niyogi P. Laplacian score for feature selection. Proceedings of the 18th International Conference on Neural Information Processing Systems; 2005; Vancouver, British Columbia, Canada.
49. Chang Y-W, Lin C-J. *Feature Ranking Using Linear SVM*. Proceedings of the Workshop on the Causation and Prediction Challenge at WCCI 2008; 2008; Proceedings of Machine Learning Research.
50. Cawley GC, Talbot NLC. Efficient leave-one-out cross-validation of kernel Fisher discriminant classifiers. *Pattern Recognition*. 2003; **36**(11): 2585–2592.
51. Hastie T, Tibshirani R, Friedman J. *The Elements of Statistical Learning*. Vol. 2. New York: Springer; 2009.
52. von Elm E, Altman DG, Egger M, Pocock SJ, Gøtzsche PC, Vandenbroucke JP, et al. The Strengthening of Reporting of Observational Studies in Epidemiology (STROBE) Statement: guidelines for reporting observational studies. *Ann Intern Med*. 2007; **147**(8): 573–577.
53. Sanz-Arigita EJ, Schoonheim MM, Damoiseaux JS, Rombouts SA, Maris E, Barkhof F, et al. Loss of 'small-world' networks in Alzheimer's disease: graph analysis of fMRI resting-state functional connectivity. *PLoS One*. 2010; **5**(11): e13788.
54. Zhou Y, Lui YW. Small-world properties in mild cognitive impairment and early Alzheimer's disease: a cortical thickness MRI study. *ISRN Geriatr*. 2013; **2013**: 542080.
55. Zald DH. Orbitofrontal cortex contributions to food selection and decision making. *Ann Behav Med*. 2009; **38**(Suppl 1): S18–S24.
56. Killgore WD, Young AD, Femia LA, Bogorodzki P, Rogowska J, Yurgelun-Todd DA. Cortical and limbic activation during viewing of high- versus low-calorie foods. *Neuroimage*. 2003; **19**(4): 1381–1394.
57. Nederkoorn C, Smulders FT, Jansen A. Cephalic phase responses, craving and food intake in normal subjects. *Appetite*. 2000; **35**(1): 45–55.
58. Rolls ET. The orbitofrontal cortex and reward. *Cereb Cortex*. 2000; **10**(3): 284–294.
59. Staresina BP, Davachi L. Differential encoding mechanisms for subsequent associative recognition and free recall. *J Neurosci*. 2006; **26**(36): 9162–9172.
60. Bookheimer S. Functional MRI of language: new approaches to understanding the cortical organization of semantic processing. *Annu Rev Neurosci*. 2002; **25**: 151–188.
61. Vandenberghe R, Price C, Wise R, Josephs O, Frackowiak RSJ. Functional anatomy of a common semantic system for words and pictures. *Nature*. 1996; **383**(6597): 254–256.
62. Zatorre RJ, Belin P, Penhune VB. Structure and function of auditory cortex: music and speech. *Trends Cogn Sci*. 2002; **6**(1): 37–46.
63. von Saldern S, Noppeney U. Sensory and striatal areas integrate auditory and visual signals into behavioral benefits during motion discrimination. *J Neurosci*. 2013; **33**(20): 8841–8849.
64. van der Laan LN, de Ridder DT, Viergever MA, Smeets PA. The first taste is always with the eyes: a meta-analysis on the neural correlates of processing visual food cues. *Neuroimage*. 2011; **55**(1): 296–303.
65. Killgore WD, Yurgelun-Todd DA. Positive affect modulates activity in the visual cortex to images of high calorie foods. *Int J Neurosci*. 2007; **117**(5): 643–653.
66. Simmons WK, Martin A, Barsalou LW. Pictures of appetizing foods activate gustatory cortices for taste and reward. *Cereb Cortex*. 2005; **15**(10): 1602–1608.
67. De Araujo IE, Rolls ET. Representation in the human brain of food texture and oral fat. *J Neurosci*. 2004; **24**(12): 3086–3093.
68. Frank GK, Reynolds JR, Shott ME, Jappe L, Yang TT, Tregellas JR, et al. Anorexia nervosa and obesity are associated with opposite brain reward response. *Neuropsychopharmacology*. 2012; **37**(9): 2031–2046.
69. Piech RM, Lewis J, Parkinson CH, Owen AM, Roberts AC, Downing PE, et al. Neural correlates of appetite and hunger-related evaluative judgments. *PLoS One*. 2009; **4**(8): e6581.
70. Thomas JM, Higgs S, Dourish CT, Hansen PC, Harmer CJ, McCabe C. Satiety attenuates BOLD activity in brain regions involved in reward and increases activity in dorsolateral prefrontal cortex: an fMRI study in healthy volunteers. *Am J Clin Nutr*. 2015; **101**(4): 697–704.
71. Siep N, Roefs A, Roebroek A, Havermans R, Bonte ML, Jansen A. Hunger is the best spice: an fMRI study of the effects of attention, hunger and calorie content on food reward processing in the amygdala and orbitofrontal cortex. *Behav Brain Res*. 2009; **198**(1): 149–158.
72. Mehta S, Melhorn SJ, Smeraglio A, Tyagi V, Grabowski T, Schwartz MW, et al. Regional brain response to visual food cues is a marker of satiety that predicts food choice. *Am J Clin Nutr*. 2012; **96**(5): 989–999.
73. Kelley AE, Baldo BA, Pratt WE, Will MJ. Corticostriatal-hypothalamic circuitry and food motivation: integration of energy, action and reward. *Physiol Behav*. 2005; **86**(5): 773–795.
74. Demos KE, Heatherton TF, Kelley WM. Individual differences in nucleus accumbens activity to food and sexual images predict weight gain and sexual behavior. *J Neurosci*. 2012; **32**(16): 5549–5552.
75. Coveleskie K, Gupta A, Kilpatrick LA, Mayer ED, Ashe-McNalley C, Stains J, et al. Altered functional connectivity within the central reward network in overweight and obese women. *Nutr Diabetes*. 2015; **5**(1): e148.
76. Wang GJ, Tomasi D, Convit A, Logan J, Wong CT, Shumay E, et al. BMI modulates calorie-dependent dopamine changes in accumbens from glucose intake. *PLoS One*. 2014; **9**(7): e101585.
77. Smeets PA, de Graaf C, Stafleu A, van Osch MJ, Niveltstein RA, van der Grond J. Effect of satiety on brain activation during chocolate tasting in men and women. *Am J Clin Nutr*. 2006; **83**(6): 1297–1305.
78. Frank S, Laharnar N, Kullmann S, Veit R, Canova C, Hegner YL, et al. Processing of food pictures: influence of hunger, gender and calorie content. *Brain Res*. 2010; **1350**: 159–166.
79. Button KS, Ioannidis JP, Mokrysz C, Nosek BA, Flint J, Robinson ES, et al. Power failure: why small sample size undermines the reliability of neuroscience. *Nat Rev Neurosci*. 2013; **14**(5): 365–376.
80. Kullmann S, Heni M, Linder K, Zipfel S, Haring HU, Veit R, et al. Resting-state functional connectivity of the human hypothalamus. *Hum Brain Mapp*. 2014; **35**(12): 6088–6096.
81. Grill HJ, Skibicka KP, Hayes MR. Imaging obesity: fMRI, food reward, and feeding. *Cell Metab*. 2007; **6**(6): 423–425.
82. Cornier MA, Von Kaenel SS, Bessesen DH, Tregellas JR. Effects of overfeeding on the neuronal response to visual food cues. *Am J Clin Nutr*. 2007; **86**(4): 965–971.